

# High-Power-Density 400VDC-19VDC LLC Solution with GaN HEMTs

Yajie Qiu, Lucas (Juncheng) Lu

GaN Systems Inc.,

Ottawa, Canada

yqiu@gansystems.com

**Abstract**—Compared to Silicon MOSFETs, GaN High-electron-Mobility Transistors (GaN HEMT) features significantly reduced gate charge ( $Q_g$ ) and output capacitance ( $C_{oss}$ ), resulting in lower driving loss and shorter deadtime. Therefore, GaN HEMTs show significant advantages over Silicon MOSFETs in high-frequency soft-switching resonant topologies such as an LLC resonant converter. With the increased switching frequency ( $F_{sw}$ ), the transformer core size can be reduced. Furthermore, 3-D PCB structure is employed to increase the power density. A 190-Watt 400V-19V (GaN Systems E-HEMT based) LLC DC-DC resonant converter is carefully designed, and the transformer is optimized for high-end adapter applications operating above 600kHz. The prototype shows a complete design with a power density over 63W/inch<sup>3</sup> (400V bus capacitor is included) while its peak efficiency has achieved 96%.

**Keywords**—GaN; HEMT; LLC; DCDC; High power density

## I. INTRODUCTION

Massive research and industry interest have been attracted to the wide-band-gap device application [1-3]. High power density is one key motivation for GaN HEMTs to be widely used in low power consumer applications such as laptop adapter, flat screen TVs, and all-in-one desktops. The LLC resonant converter topology is effective in improving efficiency, especially for high-input voltage applications where the switching loss is more dominant than the conduction loss [4-6]. The series and parallel inductors are often integrated into the transformer using the leakage and the magnetizing inductance, thus reducing the component count. The purpose of this paper is to pursue a high-power-density and high-efficiency DC-DC LLC solution using GaN HEMTs.

The design is described in four steps. 1) The capability of GaN HEMTs operating at high-frequency soft-switching LLC application is investigated. 2) “3-D PCB Structure” is introduced and implemented in the whole design to push the power density. 3) The high-frequency LLC transformer design steps and its structure is mentioned, and the transformer loss will be analyzed. 4) The key waveforms of the designed LLC topology and the test results will be shown.

## II. ADVANTAGES OF GAN IN HIGH-FREQUENCY SOFT-SWITCHING RESONANT TOPOLOGY

Compared to Silicon MOSFETs, GaN High-electron-mobility transistors (GaN HEMTs) feature significantly

reduced gate charge ( $Q_g$ ) and output capacitance ( $C_{oss}$ ), resulting in lower driving loss and shorter turning-on/off periods. Therefore, GaN HEMTs show significant advantages over Silicon MOSFETs in high-frequency soft-switching resonant topology such as the LLC resonant converter.

In order to take a closer look at the potential advantages of GaN in high-frequency soft-switching resonant converters, we have to compare the key parameters of GaN HEMTs to those of the conventional Si MOSFETs. As an example, GaN Systems’ GS55504B is selected to be compared to the Si MOSFET IPx65R110CFD because they have comparable  $R_{DS(ON)}$  values. The following table shows the comparison of the key parameters:  $V_{DS}$ ,  $R_{DS(ON)}$ ,  $Q_g$ ,  $C_{O(ER)}$  and  $C_{O(TR)}$ .

TABLE I.  $Q_g$  AND  $C_{oss}$  COMPARISON

	Si CoolMOS CFD2	GaN HEMT	Unit
	IPx65R110CFD	GS66504B	
$V_{DS}$	650	650	V
$R_{DS(ON)}$	110	110	mΩ
$Q_g$	118	3	nC
$C_{O(ER)}$	118	44	pF
$C_{O(TR)}$	582	72	pF

### A. The $Q_g$ advantage of GaN

As shown in Fig. 1, the GS55504B features significantly reduced gate charge ( $Q_g$ ) compared to the IPx65R110CFD, resulting in a lower driving loss. Fig. 2 shows the comparison of gate-driver loss at different switching frequencies. The loss difference between two devices increases dramatically with the increase of the switching frequency, demonstrating the advantage of GaN HEMTs working at the high switching frequency.

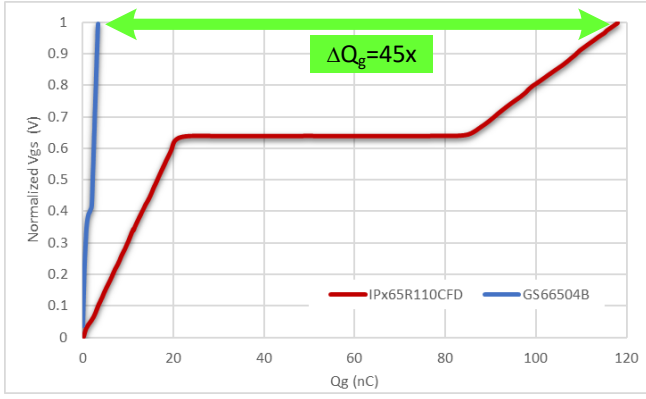


Fig. 1.  $Q_g$  comparison

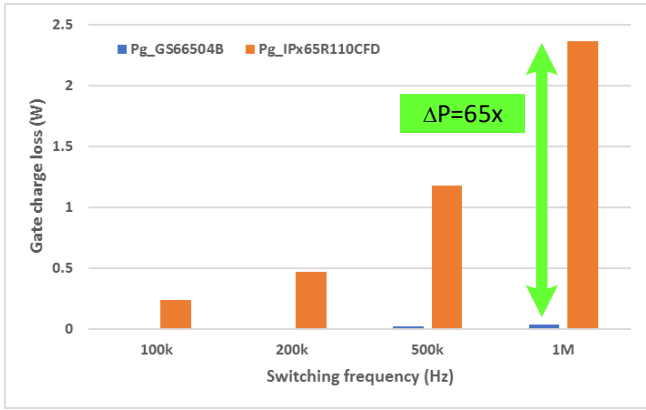


Fig. 2. Gate-driver loss comparison

### B. The $C_{oss}$ advantage of GaN

$C_{oss}$  of a Si MOSFET is highly nonlinear at low voltage. The  $C_{oss}$  values of a GaN HEMT and a Si MOSFET are compared in Fig. 3 and Fig. 4. The GaN HEMT features significantly reduced output capacitance ( $C_{oss}$ ) and  $C_{oss}$  energy, resulting in shorter turning-on/off period, as shown in Fig. 5. This characteristic allows the shorter deadtime and high switching frequency operation to be achieved.

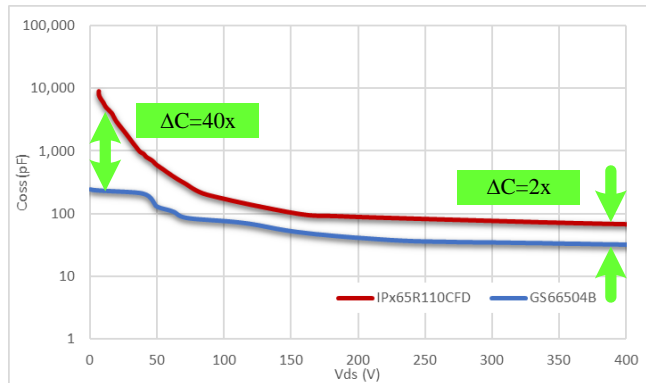


Fig. 3.  $C_{oss}$  comparison

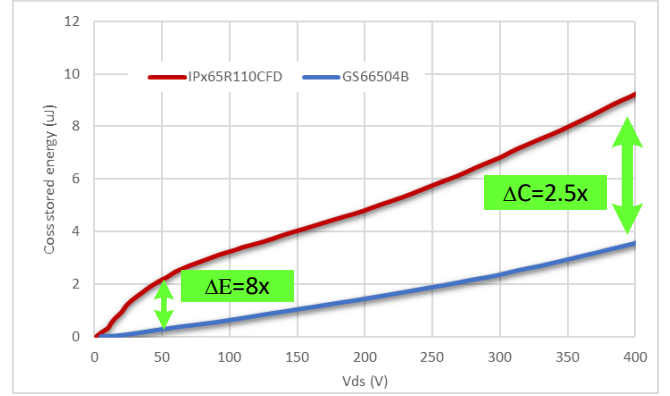


Fig. 4.  $C_{oss}$  energy comparison

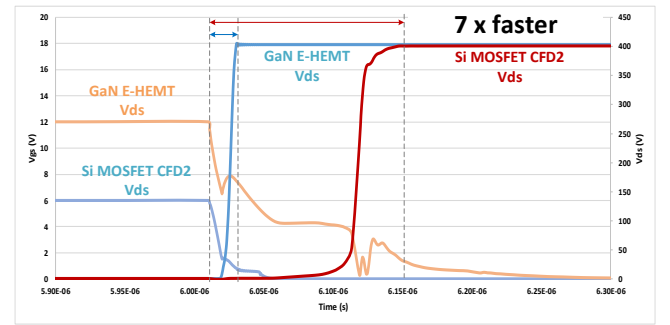


Fig. 5.  $C_{oss}$  charging time comparison at the turn-off

### C. The GaN advantage in LLC resonant converter

The schematic of GaN-based half bridge LLC converter is plotted in Fig. 6.

For the LLC resonant converter working in the below-resonance region and at-resonance point, primary side half-bridge switches,  $S_1$  and  $S_2$ , always safely turn on without incurring switching loss (Zero-voltage Switching). The total loss resulting from the power switches is composed of three parts: 1) driving loss (decided by  $Q_g$ ), 2) conduction loss (decided by  $R_{DS(ON)}$ ) and 3) switching off loss (decided by  $C_{oss}$ ). It has been analyzed that the GS55504B has the all three mentioned advantages over the Si MOSFET IPx65R110CFD when operating at high-frequency soft-switching frequency LLC converters.

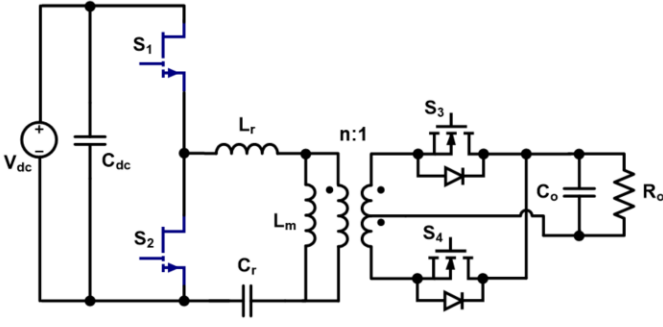


Fig. 6. GaN-based half-bridge LLC converter

The design specification of the LLC converter is shown in table II, which is very popular in two-stage adapter applications.

TABLE II. DESIGN SPECIFICATIONS

$V_{in}$	350-400	V
$V_o$	19	V
$I_o$	10	A
$P_o$	190	W

The LLC tank is designed, and the parameters are listed in Table III. A lot of documents have provided multiple methods to design the LLC resonant tank parameters, so the design process is not included in this paper.

TABLE III. LLC RESONANT TANK PARAMETERS

$L_m$	80	$\mu H$
$L_r$	5	$\mu H$
$C_r$	6	nF
$F_r$	726	kHz

### III. 3-D PCB STRUCTURE SOLUTION FOR HIGH-POWER-DENSITY LLC RESONANT CONVERTER

#### A. 3-D Structure Concept

In order to push the power density of the GaN HEMTs based LLC prototype, the “3-D PCB” concept is utilized, where all the active switches, power diodes, and MCU are assembled on the PCB daughter cards. Then these daughter cards are inserted vertically on a horizontal PCB mother board to minimize their occupied area of the PCB mother board while fully utilizing the room above. Since all the daughter cards and heatsinks are intentionally designed to be lower than the highest components on the mother board (e.g., LLC Transformer), the height of the prototype is the same as that of 2-D PCB solution.

#### B. Implementation

The whole LLC system design is composed of the following four parts:

##### 1) PCB board #1:

Primary side half-bridge daughter card with two GaN HEMTs (GS66504B) and bootstrap driving circuitry (32mm (L)  $\times$  19mm (W)). Since GS66504B are a bottom-side-cooling device, one 17mm  $\times$  17mm square shape heatsink is connected to the bottom side of PCB to cool the two GaN HEMTs.

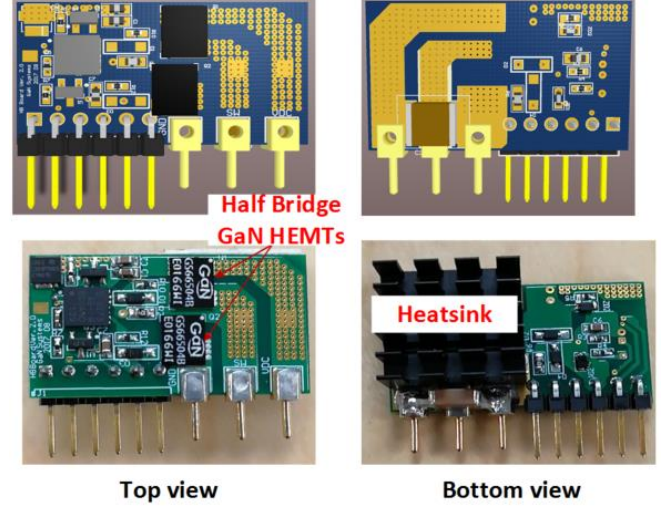


Fig. 7. Primary side half bridge daughter card PCB layout (top) and pictures (bottom)

##### 2) PCB board #2:

Primary side digital controller with peripheral circuits (26mm (L)  $\times$  20mm (W)). The topology employs a digital control solution integrating an output voltage regulation, OVP, and OCP function into one low-cost MCU (DSPIC33FJ06GS202A from Microchip).

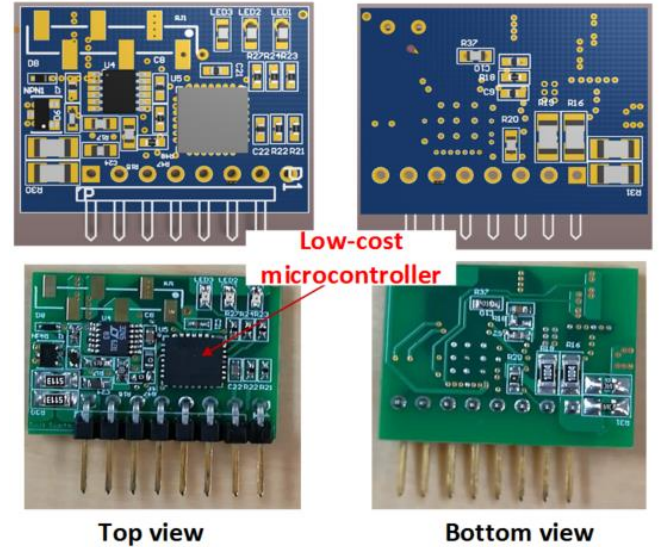




Fig. 8. Primary side digital controller daughter card PCB layout (top) and pictures (bottom)

### 3) PCB board #3:

Secondary side synchronized rectifier daughter card (20mm (L) × 17mm (W)). All the components are soldered on only the top side. One 20mm × 20mm square shape heatsink is connected to the bottom side of PCB to cool the four Synchronized Rectifier MOSFETs (2 × 2 paralleled MOSFETs).

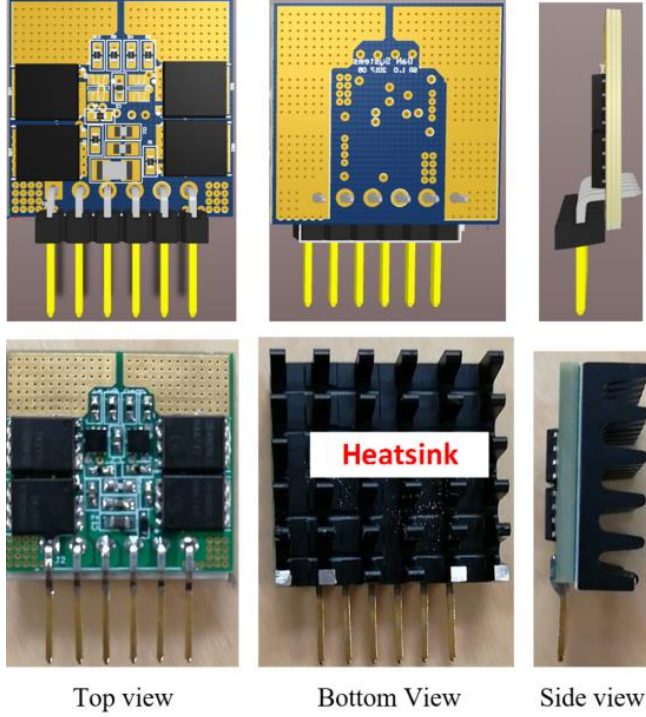


Fig. 9. Secondary side synchronized rectifier daughter card PCB layout (left) and pictures (right)

### 4) PCB board #4:

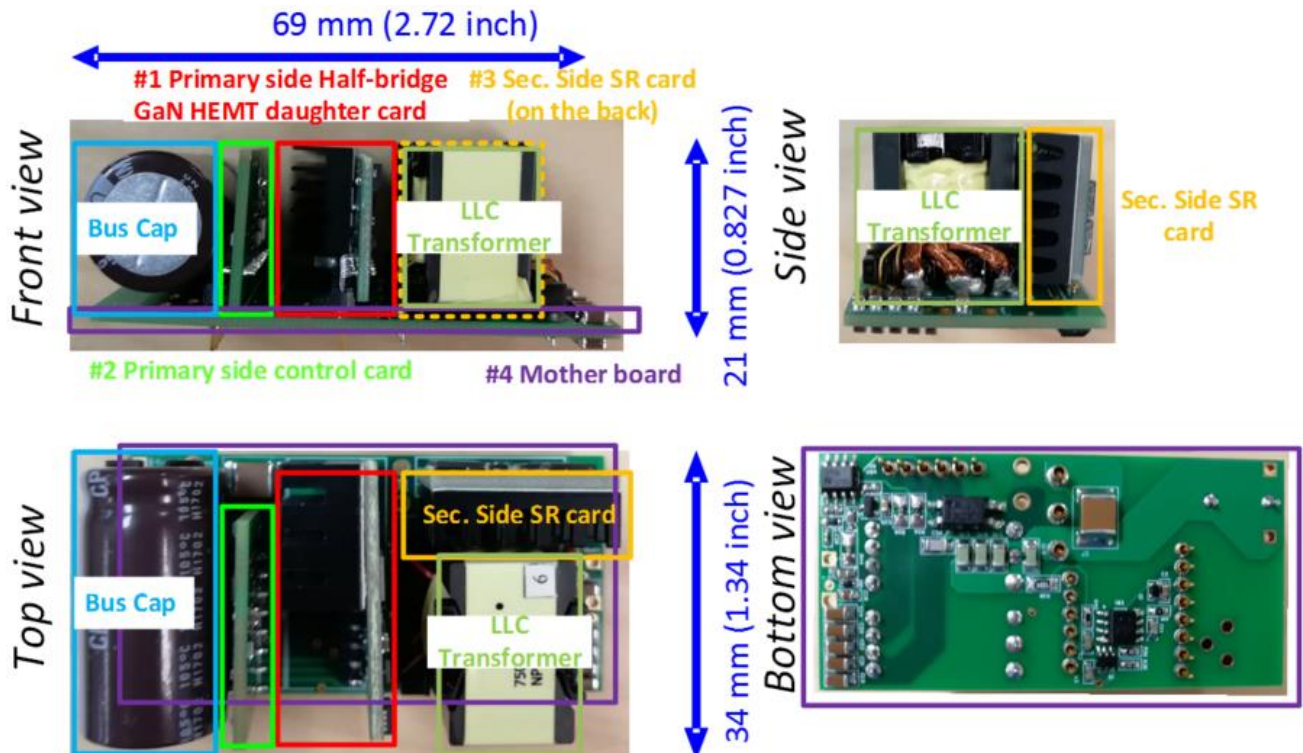
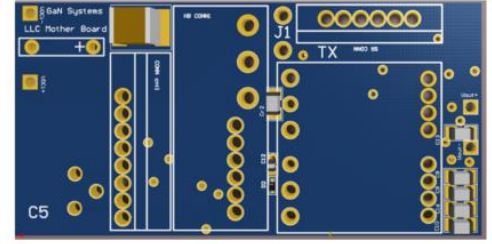
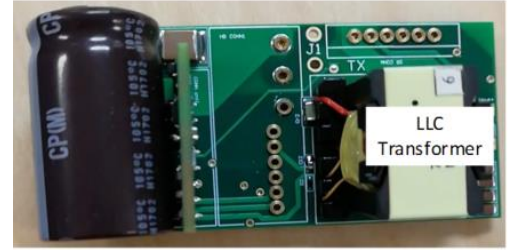


Fig. 1. Designed GaN-based LLC Resonant Converter Prototype

Mother board with input capacitor, output filter and integrated transformer (69mm (L) × 34mm (W)) is shown in Fig. 10. Three slots are provided on the mother board for PCB board #1, PCB board #2 and PCB board #3 to be inserted.



PCB layout



Mother board picture

Fig. 10. LLC Mother Board PCB layout (top) and picture (bottom)

### C. LLC prototype and its power density

The finished prototype and its dimension are shown in Fig. 11. All the heatsinks are connected to the bottom side of the daughter cards, which is effective for the bottom-side cooling devices, such as GaN HEMT, GS66504B, on the PCB board #1 and secondary side synchronized rectifiers PCB board #3. The resulting power density of the prototype is 63.3W/inch<sup>3</sup>.

$$V = 69\text{mm}(L) \times 21\text{mm}(H) \times 34\text{mm}(W) = 3 \text{ inch}^3 \quad (1)$$

$$\text{Power density} = \frac{190W}{3 \text{ inch}^3} = 63.3W / \text{inch}^3 \quad (2)$$

#### IV. THE HIGH-FREQUENCY LLC TRANSFORMER DESIGN CONSIDERATIONS AND ITS STRUCTURE

It has been explained in Part II that GaN HEMTs enable the LLC operating at the high switching frequency ( $F_{sw}$ ). With the increased switching frequency, the primary side winding turns ( $N$ ), and effective core area ( $A_e$ ) reduces. Then the transformer core size can be reduced, and the power density can be increased. The correlation between core size and  $F_{sw}$  has been shown in the following magnetic flux density ( $B$ ) equation:

$$\Delta B_{\max} = \frac{0.5 \times N \times V_o}{N_p \times A_e \times F_{sw}} \quad (3)$$

##### A. Transformer core material and bobbin selection

In order to reduce the transformer core loss, high-frequency core material TP5 is selected, whose optimal operation range is (500kHz to 1MHz). Additionally, the conventional transformer core and bobbin, PQ2020, is used in this design. Not only is it a low-cost standard product, but also the resonant inductor of the LLC tank can be easily integrated into the transformer by making use of its leakage inductance.

According to (2) and (3), the maximum of the flux density of the designed LLC transformer operating at 600kHz is 128mT. Therefore, it is within the safe operating area of TP5, as shown in Fig. 12.

$$\begin{aligned} \Delta B_{\max} @ 600kHz &= \frac{0.5 \times N \times V_o}{N_p \times A_e \times F_{sw}} \\ &= \frac{0.5 \times 11.5 \times 19V}{23 \times 62.47mm^2 \times 600kHz} = 128mT \end{aligned} \quad (4)$$

$$128mT = \Delta B_{\max} @ 600kHz \leq B_{sat} = 350mT \quad (5)$$

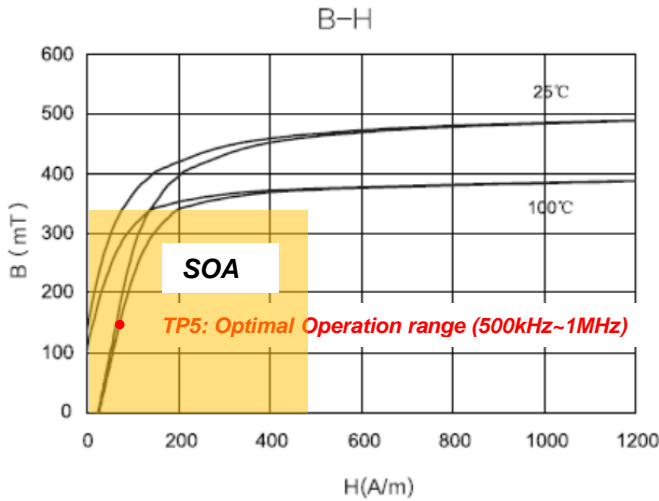


Fig. 11. B-H Curve of TP5

##### B. Turns ratio design

For the high-frequency switching mode power supply, besides the limitation of saturation flux density ( $B_{sat}$ ), the core size is also limited by the total transformer power loss and the turns ratio of the transformer.

LLC transformer turns ratio is decided by the input and output voltage to ensure the converter working at the resonant frequency under the nominal input and output voltages. For example, the application of 400V<sub>in</sub>-19V<sub>out</sub> half-bridge LLC converter requires the turns ratio shown in (4).

$$\frac{N_{pri}}{N_{sec}} = \frac{0.5 \times V_{in}}{V_{out}} = \frac{200}{19} \quad (6)$$

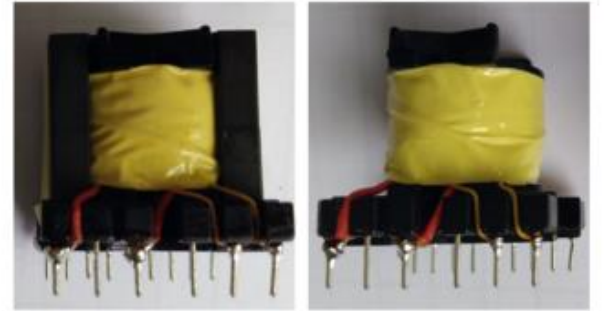
Therefore, the total winding transformer turns is  $N_{pri} + N_{sec} = 23 + 2 + 2 = 27$  turns. The detailed transformer specifications are listed in Table III.

TABLE IV. LLC TRANSFORMER SPECIFICATIONS

Po	190W (19Vdc/10Adc)
Input voltage	175 ~ 200Vpeak
Pri. to half Sec. turn ratio	23: 2: 2
Primary magnetizing inductance	80μH
Operational temperature	-40 ~ 130°C
Leakage inductance	5μH

##### C. Transformer Loss calculation

The picture of the designed transformer is shown in Fig. 12, where Fig 12.a shows the picture of the transformer and Fig 12.b shows the bobbin of the transformer with the winding.



a. With core

b. Without core

Fig. 12. Transformer picture

##### 1) Core loss:

The PQ2020 is a standard size with 2.8255cm<sup>3</sup>; the core loss can be calculated by using the  $P_{cv}$ - $B_m$  data from TP5 datasheet, as shown in (5).

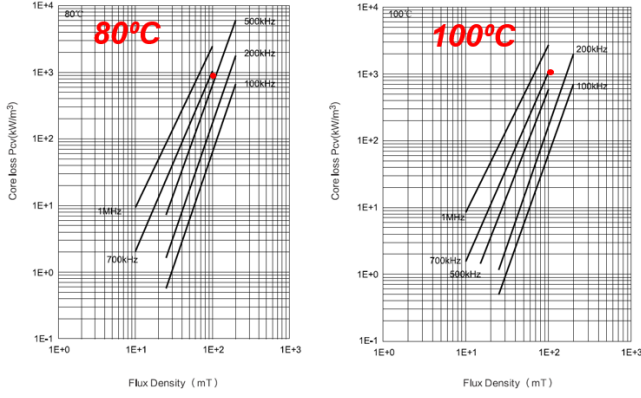


Fig. 13.  $P_{cv}$ - $B_m$  curve for TP5

$$P_{core} = P_{CV @ 200mT, 700kHz} \times V_e \quad (7)$$

$$= 90mW / cm^3 \times 2.8255cm^3 = 2.5W$$

### 2) Copper loss

The copper loss is decided by the primary side and secondary side winding resistance. Both of them grow with the increasing of operating frequency because of skin effect, as shown in Table IV.

TABLE V. TRANSFORMER WINDING RESISTANCE (TESTING RESULTS)

Operating Frequency (kHz)	Primary side winding res (Ohms)	Secondary side winding res (mOhms)
400	0.5	14
500	0.68	17
600	0.95	22.5
700	1.6	28
800	2.1	33
900	2.5	33.5
1000	2.9	49.5

It is noticed that the Primary side resistance @ 600kHz is  $0.95\Omega$  while the Secondary side resistance @ 600kHz is  $22.5m\Omega$ . The copper loss can be calculated in (6).  $I_{pri}$  and  $I_{sec}$  values are estimated by simulation at full load.

$$P_{COPPER} = (I_{pri})^2 R_{pri} + (I_{sec})^2 R_{sec} \quad (8)$$

$$= 1.3^2 \times 0.95 + 11.54^2 \times 0.0225 = 4.6W$$

### 3) Total loss

Therefore, the total loss can be calculated.

$$P_{total} = P_{core} + P_{copper} = 2.5W + 4.6W = 7W \quad (9)$$

According to the above loss analysis, the designed LLC transformer brings 7W loss (3.7% of the total output power) at full load, which is reasonable.

## V. EXPERIMENTAL RESULTS

The key waveforms of designed high-frequency LLC converter working at half load and full load are shown in Fig. 14 and Fig. 15.

It is noticed that the effective resonant frequency (623kHz @ 50% load and 617kHz @ 100% load) is lower than the calculated value (723kHz). This is because:

1) The calculated period does not include the deadtime. Effective period = calculated period + deadtime

2) There is parasitic inductance on PCB,

The effective resonant inductance,  $L_{r\_effective}$ , is larger than the transformer leakage inductance,  $L_{lk}$ :  $L_{r\_effective} = L_{lk} + L_{pcb}$

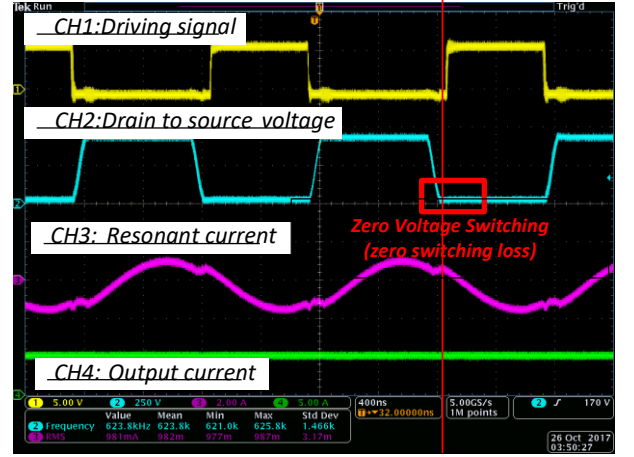


Fig. 14. The key experimental waveforms of the proposed high-power-density GaN HEMT LLC converter when  $V_{in}=400V$ ,  $V_{out}=19V$ ,  $I_o=5A$   $P_o=95W$ ,  $F_s=623kHz$  (50% load)

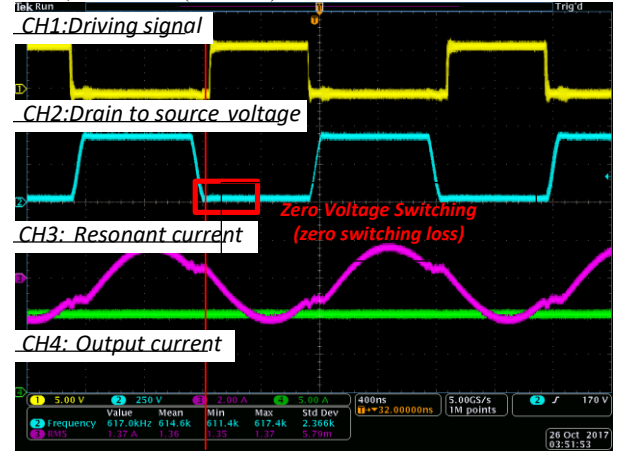


Fig. 15. The key experimental waveforms of the proposed high-power-density GaN HEMT LLC converter when  $V_{in}=400V$ ,  $V_{out}=19V$ ,  $I_{out}=10A$ ,  $P_o=190W$ ,  $F_s=617kHz$  (100% load)

The efficiency at different loads is tested and shown in Fig. 16, the power loss from the auxiliary winding is not included. The peak efficiency has achieved 96.1 at 95W (50% load) while the efficiency at 190W (100% load) is 95.6%

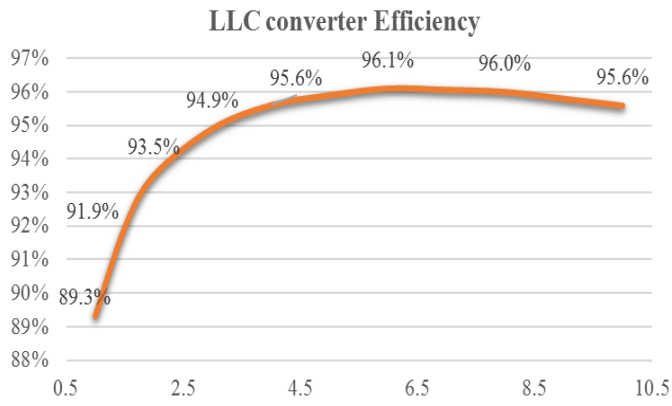


Fig. 16. The efficiency performance at different load (1A 19W to 10A 190W)

## VI. CONCLUSION

The GaN HEMTs features a superior figure of merit (low  $Q_g$ ,  $R_{DS(ON)}$  and  $C_o$ ) which enables the resonant converter such as the analyzed LLC allowing operating at a high switching frequency over 600kHz. The smaller core using high-frequency magnetic materials can then be employed to increase the power density. Furthermore, with the help of 3-D PCB structure as well as the combined digital control solution, the prototype shows a complete 400VDC-19VDC

design with a power density of 63W/inch<sup>3</sup> while its peak efficiency has achieved 96.1%.

## REFERENCES

- [1] R. Hou, J. Xu, and D. Chen, "A multivariable turn-on/turn-off switching loss scaling approach for high-voltage GaN HEMTs in a hard-switching half-bridge configuration," in *2017 IEEE 5th Workshop on Wide Bandgap Power Devices and Applications (WiPDA)*, 2017, pp. 171-176.
- [2] J. Lu, Y. Qiu, and D. Chen, "A Full Power Emulation Platform for Evaluating Power Semiconductors," presented at the Thirty-Third Annual IEEE Applied Power Electronics Conference and Exposition (APEC2018), San Antonio, Texas, March 4-8, 2018.
- [3] J. Lu, R. Hou, and D. Chen, "Opportunities and Design Considerations of GaN HEMTs in ZVS Applications," presented at the Thirty-Third Annual IEEE Applied Power Electronics Conference and Exposition (APEC2018), San Antonio, Texas, March 4-8, 2018.
- [4] Z. Hu, L. Wang, Y. Qiu, Y.-F. Liu, and P. C. Sen, "An Accurate Design Algorithm for LLC Resonant Converters Part II," *IEEE Transactions on Power Electronics*, vol. 31, no. 8, pp. 5448-5460, 2016.
- [5] Y. Qiu, L. Wang, H. Wang, Y. Liu, and P. C. Sen, "Bipolar Ripple Cancellation Method to Achieve Single-Stage Electrolytic-Capacitor-Less High-Power LED Driver," *Emerging and Selected Topics in Power Electronics, IEEE Journal of*, vol. 3, no. 3, pp. 698-713, 2015.
- [6] Y. Qiu, W. Liu, P. Fang, and Y.-F. Liu, "A Mathematical Guideline for Designing an AC-DC LLC Converter with PFC," presented at the Thirty-Third Annual IEEE Applied Power Electronics Conference and Exposition (APEC2018), San Antonio, Texas, March 4-8, 2018.